Int. J. Heat Mass Transfer. Vol. 29, No. 9, pp. 1349–1357, 1986
Printed in Great Britain

0017–9310/86 $3.00 + 0.00
Pergamon Journals Ltd.

Frequency response of boiling flow systems based on a two-fluid model

R. P. ROY,* M.-G. SU,* R. C. DYKHUIZEN† and S. P. KALRA‡

*Department of Mechanical and Aerospace Engineering, Arizona State University, Tempe, AZ 85287, U.S.A.
† Fluid and Thermal Sciences Department, Sandia National Laboratories, Albuquerque, NM 87185, U.S.A.
‡ Nuclear Power Division, Electric Power Research Institute, Palo Alto, CA 94304, U.S.A.

(*Received* 20 *September* 1985 *and in final form* 16 *January* 1986)

Abstract—A distributed parameter model of boiling flow systems in the frequency domain is presented. It is constructed from a linearized time domain, two-fluid model by the state-space vector method. To demonstrate the validity of this approach, transfer functions calculated by the present model are compared with analytical solutions and experimental measurements.

INTRODUCTION

THE OBJECTIVE of this work was to develop a distributed parameter model of boiling flow systems in the frequency domain beginning with a linearized time domain, two-fluid model of such systems which was already available [1]. The state-space vector method [2] was to be used and the calculated frequency responses were to be compared with experimental data [3, 4] as well as with calculation results obtained by another group on the basis of the drift-flux model formulation of two-phase flow [5]. Furthermore, the frequency response of an all-liquid flow channel calculated by the limiting form (as the vapor fraction tends to zero) of the distributed parameter model was to be compared with a closed-form analytic lumped parameter description of the same.

A modest amount of work encompassing analysis and experiments has been reported on the frequency response of boiling flow systems. Of these, two experimental studies [3, 4] and one analysis [5] have already been mentioned. Zuber and Staub reported their findings, based on analyses and experiments, on the transient response (including frequency response) of boiling flow systems [6, 7]. The analyses were based on the drift-flux model of boiling flow. Paul *et al.* investigated the frequency response of boiling flow in channels both experimentally and analytically [8]. Their distributed parameter model was also based on the drift-flux formulation of boiling flow. Several papers presented at the symposium on two-phase flow dynamics in Eindhoven, The Netherlands, reported frequency response results (e.g. [9]). In addition, a few frequency domain analyses of dynamic instability in vapor–liquid flow systems based on the drift-flux formulation are available in the literature (e.g. [5, 10]).

The contribution of the present work lies in the computation technique used for obtaining frequency response results. We show that the frequency response calculations can essentially be reduced to matrix operations in the computer in the event of a time-domain model of the system being available. Tiresome (and error-prone) algebra generally associated with obtaining expressions for various transfer functions is virtually eliminated in our approach.

TWO-FLUID MODEL OF BOILING FLOW

I. *Phase conservation equations*

The time- and cross-sectional area-averaged equations for the phase k (k = G for vapor, k = L for liquid), written per unit mixture volume, are [11, 12]:

Mass

$$\frac{\partial}{\partial t}[\langle\alpha_k\rangle_2\bar{\bar{\rho}}_k] + \frac{\partial}{\partial z}[\langle\alpha_k\rangle_2\bar{\bar{\rho}}_k\langle\bar{\bar{u}}_{kz}\rangle_2] = \langle\Gamma_k\rangle_2 \quad (1)$$

z-Momentum

$$\frac{\partial}{\partial t}[\langle\alpha_k\rangle_2\bar{\bar{\rho}}_k\langle\bar{\bar{u}}_{kz}\rangle_2] + \frac{\partial}{\partial z}[C_k\langle\alpha_k\rangle_2\bar{\bar{\rho}}_k\langle\bar{\bar{u}}_{kz}\rangle_2^2] = -\langle\alpha_k\rangle_2\frac{\partial\bar{\bar{p}}}{\partial z} + \underbrace{\frac{P_w}{A_{x-s}}\alpha_{kw}\tau_{w,z}}_{\text{wall friction}} + g_z\rho_k\langle\alpha_k\rangle_2 + \langle\Gamma_k u_{kI,z}\rangle_2 + \underbrace{F^k_{ID,z}}_{\text{interfacial drag}}$$

$$\underbrace{\pm\bar{\mu}\langle\alpha_d\rangle_2\langle\alpha_c\rangle_2\bar{\bar{\rho}}_c\left[\frac{\partial}{\partial t}(\langle\bar{\bar{u}}_{dz}\rangle_2 - \langle\bar{\bar{u}}_{cz}\rangle_2) + \langle\bar{\bar{u}}_{dz}\rangle_2\cdot\frac{\partial}{\partial z}(\langle\bar{\bar{u}}_{dz}\rangle_2 - \langle\bar{\bar{u}}_{cz}\rangle_2)\right]}_{\text{added mass effect§}} \quad (2)$$

§This is one of several expressions that have been suggested for the added mass term (e.g. [13, 14]).

NOMENCLATURE

$A_{x\text{-}s}$	cross-sectional area of flow channel [m^2]
A_w	cross-sectional area of heated channel wall [m^2]
C_k	distribution parameter, equation (5)
C_w	specific heat of wall material [J kg^{-1} K^{-1}]
$\bar{\bar{f}}_k$	k-phase time-average of variable f_k
$\langle f_k \rangle_2$	cross-sectional, area-averaged value of variable f_k
g_z	gravitational acceleration in z-direction [m s^{-2}]
h_k	enthalpy per unit mass of phase k [J kg^{-1}]
K	orifice pressure drop coefficient $\triangleq \Delta p/\frac{1}{2}\rho u^2$
$1/L_s$	interfacial (G–L) area concentration [m^2 m^{-3}]
p	pressure [Pa]
P_w	wetted perimeter [m]
P_h	heated perimeter [m]
q''_{kI}	interfacial heat flux [W m^{-2}]
q''_w	wall heat flux [W m^{-2}]
q'''_w	volumetric heat generation rate in channel wall [W m^{-3}]
q''_{wk}	heat flux from wall to phase k [W m^{-2}]
q''_{wI}	heat flux from wall to G–L interface [W m^{-2}]
t	time [s]
$\mathbf{u}$	input vector
u_{kz}	k-phase velocity, z-component [m s^{-1}]
$\mathbf{x}$	state vector
z	axial coordinate [m].

Greek symbols

α_k	k-phase fraction
ρ_k	k-phase density [kg m^{-3}]
Γ_k	mass generation rate, per unit mixture volume, of phase k [kg m^{-3} s^{-1}]
$\tau_{w,z}$	wall friction force in z-direction per unit wetted area [N m^{-2}].

Other subscripts

0	denotes base flow condition value.

Internal energy

$$\frac{\partial}{\partial t}[\langle\alpha_k\rangle_2\bar{\bar{\rho}}_k\bar{\bar{h}}_k]+\frac{\partial}{\partial z}[\langle\alpha_k\rangle_2\bar{\bar{\rho}}_k\bar{\bar{h}}_k\langle\bar{\bar{u}}_{kz}\rangle_2]$$
$$=\frac{\bar{\bar{q}}''_{wk}P_h}{A_{x\text{-}s}}+\langle\alpha_k\rangle_2\frac{\partial\bar{\bar{p}}}{\partial t}+\langle\bar{\bar{\alpha}}_k\rangle_2\langle u_{kz}\rangle_2\frac{\partial\bar{\bar{p}}}{\partial z}$$
$$+\langle\Gamma_k\bar{\bar{h}}_{kI}\rangle_2+\underbrace{\left\langle\frac{\bar{\bar{q}}''_{kI}}{L_s}\right\rangle_2}_{\substack{\text{interfacial (G–L)}\\ \text{heat transfer rate}}}. \quad (3)$$

In the preceding equations, uniform k-phase density and enthalpy over the channel cross-section have been assumed. The following definitions have been introduced:

$$\langle\bar{\bar{u}}_{kz}\rangle_2(z,t)\triangleq\frac{\langle\alpha_k(\mathbf{r},t)\bar{\bar{u}}_{kz}(\mathbf{r},t)\rangle_2}{\langle\alpha_k\rangle_2(z,t)} \quad (4)$$

$$C_k(z,t)\triangleq\frac{\langle\alpha_k\bar{\bar{u}}_{kz}^2\rangle_2}{\langle\alpha_k\rangle_2\langle\bar{\bar{u}}_{kz}\rangle_2^2} \quad (5)$$

The single-phase liquid or single-phase vapor conservation equations are obtained by assigning the value of unity to the appropriate phase fraction (α_G or α_L). Furthermore, no G–L interfacial terms will be present.

For the sake of clarity, we henceforth dispense with the symbols of time averaging and cross-sectional-area averaging.

II. *Heated channel wall energy equation*

The channel wall (considered thin and a good heat conductor) temperature is assumed to be radially uniform, and the wall material properties are assumed to be constant. Per unit length of channel:

$$A_wP_wC_w\cdot\frac{\partial T_w(z,t)}{\partial t}=A_wq'''_w(z)-P_hq''_w(z,t). \quad (6)$$

Note that equation (6) is written such that there is a certain lumped representation in the axial direction also. This lumping is to be across each finite-difference cell only (see Solution Scheme I).

Equations (1)–(3) and (6) comprise the nonlinear governing equations for the system.

III. *Interfacial (G–L) transfer equations*

The equations are reduced to:

Mass

$$\sum_{k=G,L}\Gamma_k=0. \quad (7)$$

z-Momentum

$$u_{kI,z}=u_{I,z} \quad (8)$$

where $u_{I,z}$ is the 'intrinsic axial velocity' of mass generation [15].

Internal energy

The equation is (Fig. 1):

$$\sum_{k=G,L}\Gamma_kh_{kI}=-\sum_{k=G,L}\frac{q''_{kI}}{L_s}+\frac{q''_{wI}}{L_s}. \quad (9)$$

Postulating that the G–L interface(s) will always be at saturation condition:

$$h_{kI}=h_{sat}(z). \quad (10)$$

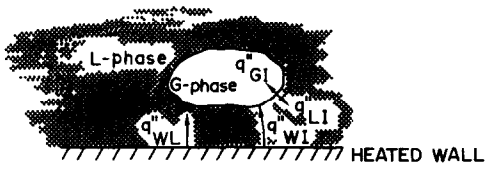

FIG. 1. Wall and interfacial heat fluxes.

Thus, equation (9) permits calculation of Γ_k if the interfacial heat fluxes and area concentrations are known.

IV. *The flow regime map and associated criteria*

Figure 2 shows the simple flow regime description incorporated in the present model. The associated criteria are as follows:

—for onset of nucleate boiling (ONB), the wall superheat criterion proposed by Sato and Matsumura [16] is adopted;

—for the net vapor generation (NVG) location, the liquid bulk subcooling criterion due to Saha and Zuber [17] is adopted;

—bubbly flow is postulated to exist between the NVG location and $\alpha_G = \alpha_{annular}$. No slug flow regime is included. Between $\alpha_G = \alpha_{annular}$ and an α_G so large that nucleate boiling can no longer be sustained at the wall because of the thinness of the liquid film (forced convection evaporation begins here), a vapor core exists along with an annular liquid film at the wall interspersed with vapor bubbles. The value of $\alpha_{annular}$ (where the vapor core begins) has been treated as an adjustable parameter between 0.40 and 0.55 in our model. Calculation results reported in this paper correspond to $\alpha_{annular} = 0.55$;

—a critical vapor velocity proposed by Steen and Wallis [18] is adopted for initiation of liquid droplet entrainment into the vapor core;

—wall dryout (or CHF) is considered to occur at an equilibrium quality based on the critical heat flux correlation due to Macbeth [19].

V. *Other constitutive equations*

Constitutive equations for wall friction, interfacial drag, wall heat transfer, interfacial heat transfer and interfacial area concentration are included. Many of these are flow regime-dependent. These have been described in detail in ref. [1] and will not be repeated here for brevity.

Thermodynamic and transport properties of steam and water have been based on relations from TRAC reports (e.g. [20, 21]).

THE SOLUTION SCHEME

I. *The linearized time-domain equations*

The partial differential equations (1)–(3) and (6) are converted into ordinary differential equations with time (t) as the only independent variable by finite differencing with respect to the axial (z) coordinate. The flow system is subdivided into discrete cells (i; $i = 1, 2, \ldots, N$) and finite differencing of the equations is performed in accordance with the second upwind (donor cell) scheme [22]. This yields the nonlinear

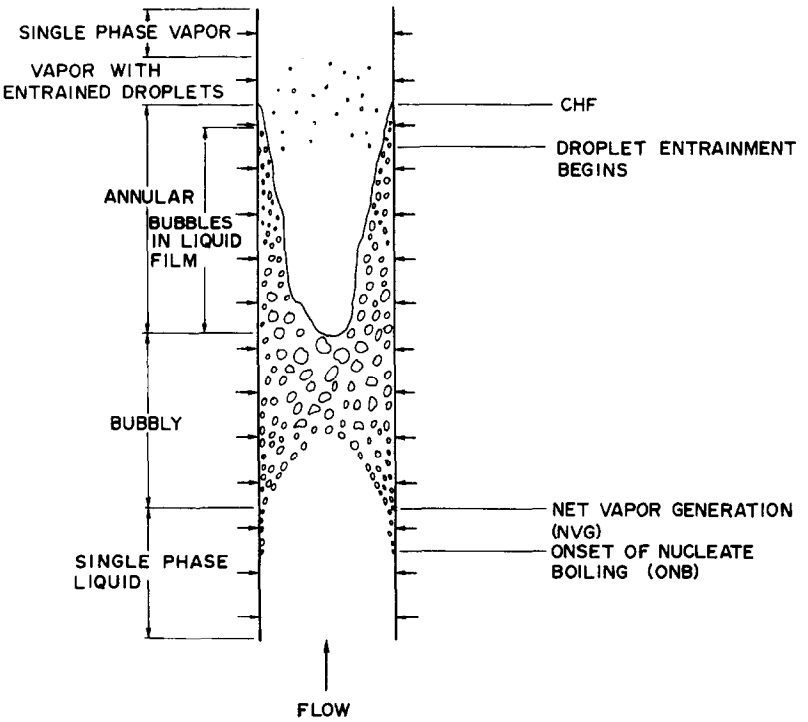

FIG. 2. The flow regimes considered.

state equation set:

$$\mathbf{M}(\mathbf{x})\dot{\mathbf{x}} = \mathbf{f}(\mathbf{x}, \mathbf{u}) \tag{11}$$

where $\mathbf{x}$ is the state vector

$$[\ldots, T_{w_i} \quad p_i \quad h_{G_i} \quad h_{L_i} \quad \alpha_{G_i} \quad u_{G_i} \quad u_{L_i}, \ldots]^T \tag{12}$$

and $\mathbf{u}$ is the input vector.

For prescribed inputs ($\mathbf{u} = \mathbf{u}_0$; e.g. heat input rate, valve and other restrictions in the flow system) and boundary conditions, the steady-state operating point of the system, $\mathbf{x}_0$, is evaluated from:

$$\mathbf{0} = \mathbf{f}(\mathbf{x}_0, \mathbf{u}_0). \tag{13}$$

The numerical method used to solve this set of simultaneous nonlinear algebraic equations has been described in detail elsewhere [23].

Next, equation set (11) is linearized, by the small perturbation technique, around the steady-state operating point $\mathbf{x}_0$ to yield:

$$\mathbf{M}_0 \frac{\mathrm{d}(\delta \boldsymbol{x})}{\mathrm{d}t} = \boldsymbol{N}_0 \delta \boldsymbol{x} + \boldsymbol{Q}_0 \delta \boldsymbol{u} \tag{14}$$

where $\delta\mathbf{x}$ is the perturbation state vector. The elements of the matrix $\boldsymbol{M}_0$ are easily calculated analytically. The elements of the matrices $\boldsymbol{N}_0$ and $\boldsymbol{Q}_0$ (these are Jacobians) are evaluated numerically by the computer.

II. *Frequency response in state space*

(i) *The forcing functions or inputs.* These are represented by the vector $\delta\mathbf{u}$ in equation (14). For simplicity of discussion, let us consider a flow system in which a single input is allowed. As an example, for a flow channel with volumetric heat generation in the wall let us adopt the wall volumetric heat generation rate, $\delta Q'''$, as the scalar input. Equation (14) then becomes:

$$\boldsymbol{M}_0 \frac{\mathrm{d}(\delta \mathbf{x})}{\mathrm{d}t} = \boldsymbol{N}_0 \delta \mathbf{x} + \mathbf{Q}_0 \delta Q'''. \tag{15}$$

In order to determine the frequency response of this system, we adopt a sinusoidal input with unity amplitude:

$$\delta Q'''(\omega) = \sin \omega t. \tag{16}$$

Since the system represented by equation (15) is linear and stationary, the state variable responses will also be sinusoidal with the same frequency. Therefore, for the jth state variable,

$$\delta x_j(\omega) = \alpha_j \sin \omega t + \beta_j \cos \omega t \tag{17}$$

where α_j and β_j are to be determined.

Let $\quad \alpha_j = c_j \cos \phi_j, \quad$ and $\quad \beta_j = c_j \sin \phi_j.$

This yields

$$\delta x_j(\omega) = c_j \sin(\omega t + \phi_j) \tag{18}$$

(ii) *The block diagram.* With the above input perturbation and output (response) signals, the system can be represented as:

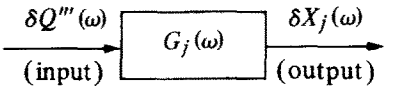

Scheme 1.

The transfer function of the system for the jth state variable, $G_j(\omega)$, is given by, from equations (16) and (18),

$$G_j(\omega) = \frac{\delta x_j(\omega)}{\delta Q'''(\omega)} = \frac{c_j \sin(\omega t + \phi_j)}{\sin \omega t}. \tag{19}$$

The magnitude of

$$G_j(\omega) = c_j = (\alpha_j^2 + \beta_j^2)^{1/2} \tag{20}$$

and the phase of

$$G_j(\omega) = \phi_j = \tan^{-1} \frac{\beta_j}{\alpha_j}. \tag{21}$$

(iii) *Determination of transfer functions.* Equation (17) can be written in vector form as:

$$\delta \mathbf{x}(\omega) = [\boldsymbol{\alpha}, \boldsymbol{\beta}] \begin{bmatrix} \sin \omega t \\ \cos \omega t \end{bmatrix} = \begin{bmatrix} \alpha_1 & \beta_1 \\ \alpha_2 & \beta_2 \\ \vdots & \vdots \\ \alpha_n & \beta_n \end{bmatrix} \begin{bmatrix} \sin \omega t \\ \cos \omega t \end{bmatrix} \tag{22}$$

Substituting equations (22) and (16) into equation (15), we obtain:

$$[\omega^2 \boldsymbol{M}_0 + \boldsymbol{N}_0(\boldsymbol{M}_0^{-1}\boldsymbol{N}_0)]\boldsymbol{\alpha} = -\boldsymbol{N}_0 \boldsymbol{M}_0^{-1} \mathbf{Q}_0 \tag{23}$$

$$[\omega^2 \boldsymbol{M}_0 + \boldsymbol{N}_0(\boldsymbol{M}_0^{-1}\boldsymbol{N}_0)]\boldsymbol{\beta} = -\omega \mathbf{Q}_0. \tag{24}$$

These specific forms of equations (23) and (24) were chosen for two reasons. First, solution of these did not involve the calculation of $\boldsymbol{N}_0^{-1}$ which was computationally difficult. Second, the LHS coefficient matrix was often found to be ill-conditioned in the other forms tried, i.e. the matrix was often very close to being singular. This meant that small changes in the matrix elements would produce large changes in the solution. On the other hand, solution of equations (23) and (24) were relatively problem-free.

From equations (23) and (24), we can calculate α_j and β_j for any state variable δx_j of interest. These can then be substituted into equations (20) and (21) to obtain the magnitude c_j and the phase ϕ_j of the transfer function $G_j(\omega)$, and a Bode diagram drawn.

Although the preceding analysis pertains to a single input only, it can be generalized to vector input [2]:

Let

$$\delta \mathbf{u}(\omega) = [\delta \mathbf{u}_1, \delta \mathbf{u}_2] \begin{bmatrix} \sin \omega t \\ \cos \omega t \end{bmatrix} \tag{25}$$

where $\delta\mathbf{u}_1$ and $\delta\mathbf{u}_2$ are prescribed r-vectors. These are converted into n-vectors by

$$Q_0\delta\mathbf{u}_1 = \mathbf{b}_1, \quad Q_0\delta\mathbf{u}_2 = \mathbf{b}_2. \tag{26}$$

Therefore, from equations (25) and (26)

$$Q_0\delta\mathbf{u}(\omega) = [\mathbf{b}_1, \mathbf{b}_2]\begin{bmatrix}\sin\omega t\\ \cos\omega t\end{bmatrix}. \tag{27}$$

Substituting equation (27) into equation (14) and proceeding as in the previous analysis, the required transfer functions can be obtained.

CALCULATION RESULT

Frequency response calculations for several flow systems were carried out. For brevity, results for only two will be presented here.

I. *An all-liquid flow system*

Figure 3 is a schematic of a part of the system. It is hydrodynamically isolated from the rest of the system via prescription of constant pressure boundary conditions at inlet and outlet. No external heat input is provided. An input perturbation is introduced in the form of a sinusoidally oscillating valve in the inlet section. This is tantamount to introducing an oscillatory perturbation in the pressure immediately downstream of the valve (i.e. immediately upstream of the test section). We wish to calculate the following 'transfer ratio':*

$$\frac{\text{test section inlet flow rate}}{\text{test section inlet pressure}}. \tag{28}$$

This is represented in the frequency domain by:

$$\frac{\delta u_{L_2}(j\omega)}{\delta p_2(j\omega)}. \tag{29}$$

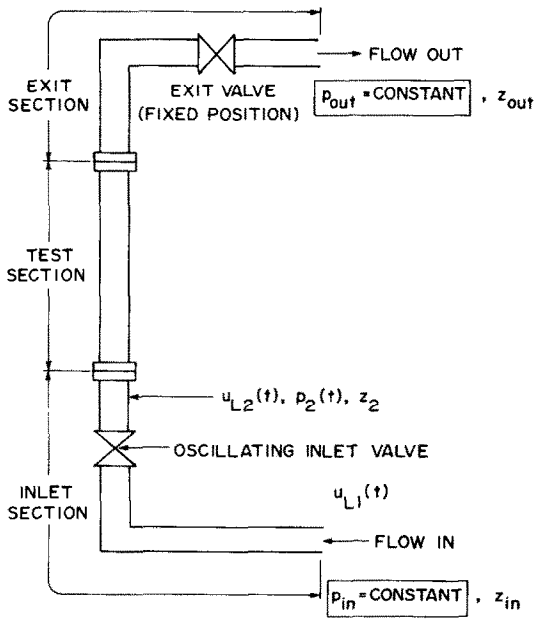

FIG. 3. An all-liquid flow system.

An analytical expression for the transfer ratio. Assuming the liquid to be incompressible, we integrate the liquid axial momentum equation over the region between the test section inlet (i.e. the oscillating valve exit) and the system exit to obtain:

$$\left[\rho_L A_{x\text{-}s}\sum_i \frac{L_i}{A_i}\right]\frac{du_{L_2}}{dt} = (p_2 - p_{out}) - \rho_L g\Delta z - \frac{1}{2}\rho_L A_{x\text{-}s}^2 u_{L_2}^2 \sum_i \frac{K_i}{A_i^2} \tag{30}$$

where

ρ_L = density of liquid,
$A_{x\text{-}s}$ = flow area of the test section,
p_2 = test section inlet pressure
L_i = length of section i,
A_i = flow area of section i,
K_i = frictional pressure drop coefficient of section i,
u_{L_2} = test section inlet flow velocity,

$$\sum_i \frac{L_i}{A_i} = \frac{L_{\text{test section}}}{A_{\text{test section}}} + \sum_{\substack{\text{exit}\\ \text{section}}} \frac{L_i}{A_i},$$

$$\sum_i \frac{K_i}{A_i^2} = \frac{K_{\text{test section}}}{A^2_{\text{test section}}} + \frac{K_{\text{exit valve}}}{A^2_{\text{test section}}} + \sum_{\substack{\text{exit}\\ \text{section}}} \frac{K_i}{A_i^2}.$$

$\Delta z =$ $(z_{out} - z_2)$, the vertical elevation of this portion of the system.

Linearizing equation (30) by the small perturbation technique and taking the Laplace transform of the resulting equation, the desired transfer ratio can be obtained:

$$\frac{\delta u_{L_2}(j\omega)}{\delta p_2(j\omega)} = \left[\frac{1}{A_{x\text{-}s}X}\right] \Big/ \left[j\omega + \frac{Y}{X}\right] \tag{31}$$

where

$$X = \rho_L \sum_i \frac{L_i}{A_i}$$

and

$$Y = \rho_L A_{x\text{-}s} u_{L_{2,0}} \sum_i \frac{K_i}{A_i^2}.$$

The gain and the phase of this transfer ratio was calculated for various frequencies and are shown by the solid lines in Fig. 4 for the following base flow

* The name 'transfer ratio' is more appropriate than 'transfer function' here because we are calculating the ratio of the responses of two state variables to inlet valve oscillation.

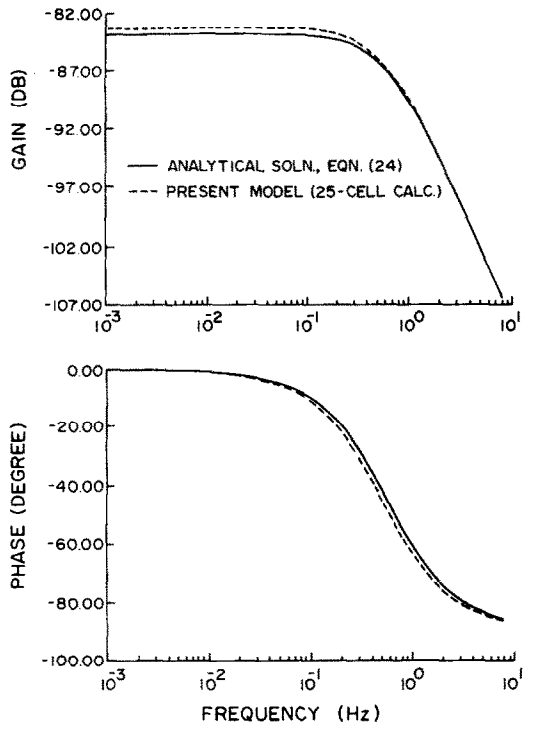

FIG. 4. Gain and phase of the transfer ratio ($\delta u_{L_2}/\delta p_2$) for an all-liquid flow system.

condition:

$$\text{Fluid} = \text{water}$$

$$\text{Heat input} = 0$$

$$p_{in} = 5\,\text{MPa}$$

$$u_{L_{1,0}} = 1.8259\,\text{m s}^{-1}$$

$$T_{in} = 532.67\,\text{K}$$

$$\sum_i \frac{L_i}{A_i} = 381.5\,\text{m}^{-1}$$

$$L_{\text{test section}} = 4.37\,\text{m}$$

$$A_{\text{test section}} = A_{\text{x-s}} = 0.014282\,\text{m}^2$$

$$K_{\text{test section}} = 1.0$$

$$K_{\text{exit valve}} = 1.0$$

$$\sum_{\substack{\text{exit}\\ \text{section}}} \frac{K_i}{A_i^2} = 14.815\,\text{m}^{-4}$$

Numerical calculation of the same transfer ratio by the present model. The all-liquid (single-phase) version of the two-fluid model equations was used to calculate the same transfer ratio numerically. This was obtained by setting the liquid fraction to unity, and setting all interfacial (G–L) terms to zero. A 25-cell representation of the flow system was employed. The calculated gain and phase are depicted by dashed lines in Fig. 4. Agreement with the results obtained from equation (30) is quite good.

Table 1. Experiment No. 313024

Inlet mass flux	864.5 kg m^{-2} s^{-1}
Exit pressure	4.97 MPa
Inlet subcooling	5.0 K
Heat input rate (per unit volume of rod)	6.26×10^7 W m^{-3}
Inlet orifice pressure drop coefficient (K_{in})	13.9

II. *The experimental system of FRIGG-2* [3]

The FRIGG test facility consisted of a 36-rod, electrically heated bundle, a riser, a steam separator, a downcomer, a spray condenser, a pump and the connecting pipes. The loop is shown schematically in Fig. 5. In the natural circulation tests, the pump section was bypassed completely.

The rod bundle test section simulated a full-scale boiling heavy-water reactor fuel element. Each rod had a 4.375-m heated length and a 13.8-mm O.D. The bundle also included a 20-mm unheated center rod to support eight prototype core spacers. The rods were mounted within a 159.6-mm-diameter shroud. The system pressure control was via regulation of cold water flow to the spray nozzle of the condenser.

All results presented in this section pertain to the natural circulation flow loop (i.e. the pump is bypassed).

The steady-state cross-sectional-average vapor fraction had been measured at seven axial locations in the test section for the experimental conditions listed in Table 1, among others.

The experimental data and the calculated vapor fraction profile based on the present model are shown in Fig. 6. The agreement is satisfactory.

In frequency response tests, measurements of the 'heating power to test section inlet flow rate' transfer function, $\delta u_{L_1}(\omega)/\delta Q'''(\omega)$, had been performed by introducing square and pseudo-random perturbations in the input power to the rod bundle. The nominal experimental condition for one of the natural circulation tests is given in Table 2.

The two-fluid model transfer function calculation results based on a 25-cell representation of the natural circulation loop are shown in Fig. 7 for two different values of inlet piping inertia parameter $\Sigma_{in} L_i/A_i$. The experimentally measured gain and phase of the transfer function are also shown in Fig. 7. The agreement is satisfactory.

Table 2. Experiment No. 362016

Inlet mass flux	886 kg m^{-2} s^{-1}
Exit pressure	5.0 MPa
Inlet subcooling	4.6 K
Heat input rate (per unit volume of rod)	1.20×10^8 W m^{-3}
Inlet orifice pressure drop coefficient (K_{in})	14.0

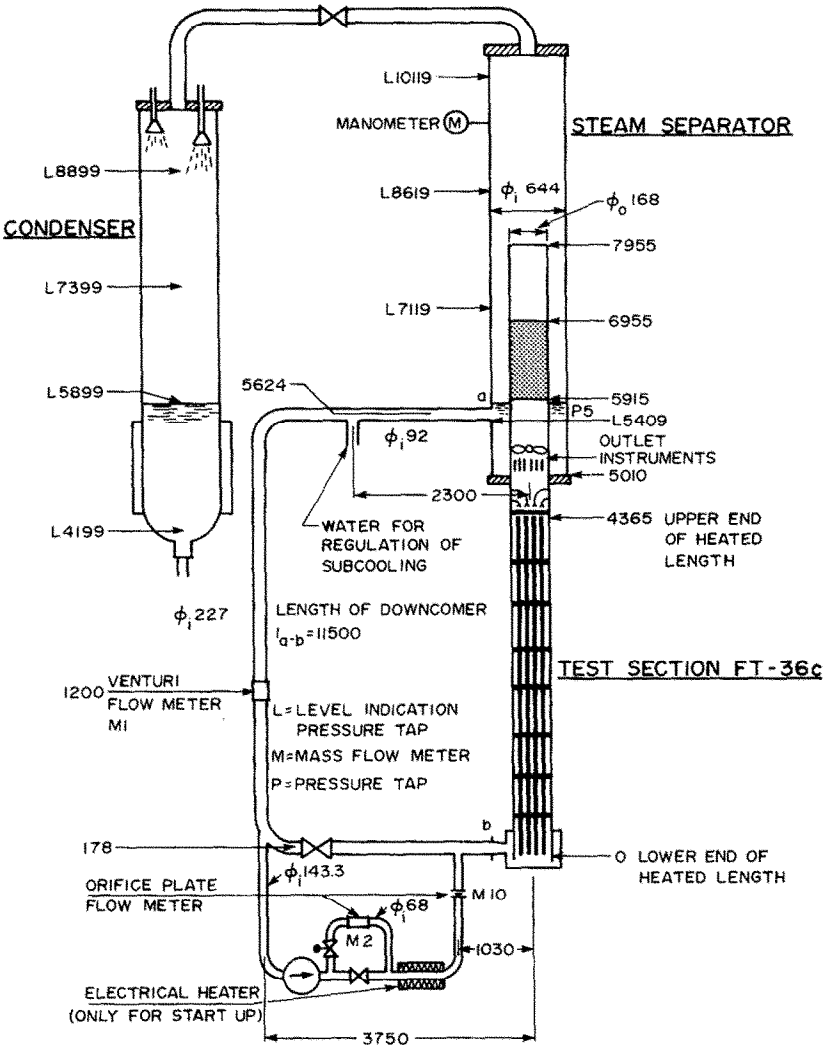

FIG. 5. The FRIGG experimental loop, data in mm [3].

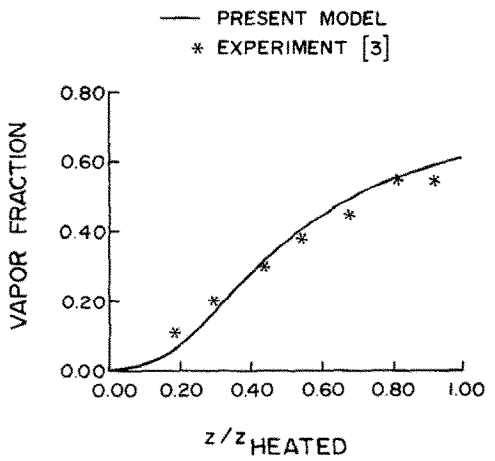

FIG. 6. Steady-state vapor fraction profile along the test section for Experiment No. 313024 [3].

Earlier experiments carried out in the FRÖJA loop [3] indicated that at the frequency corresponding to the maximum gain, the phase was close to 180°. Our computational results agree with this behavior.

A frequency response model based on the drift-flux model description of two-phase flow has recently been developed by Park *et al.* [5]. Results obtained by this model for the same experiment are also shown in Fig. 5.

Comparisons of calculation results based on the present model with other FRIGG-2 frequency response tests [3] and tests run at Argonne National Laboratory [4] also proved to be satisfactory [24].

CONCLUDING REMARKS

The major advantage of the methodology used in this work over those adopted in earlier frequency

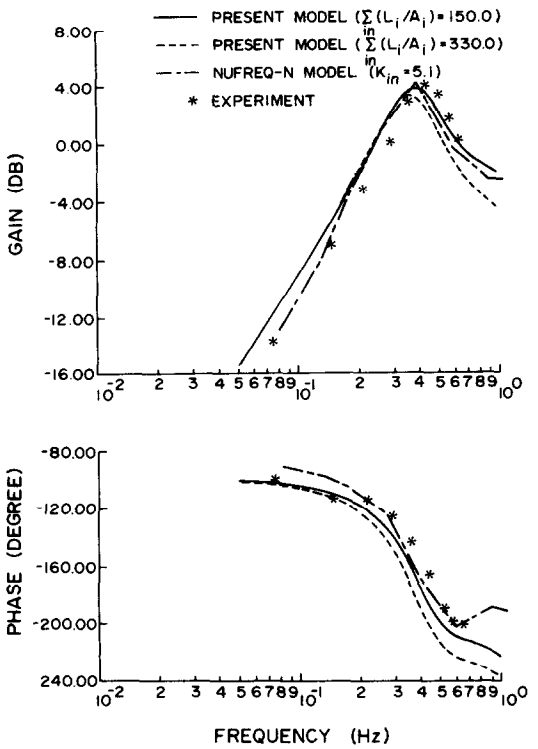

FIG. 7. Gain and phase of the transfer function ($\delta u_{L_i}/\delta Q'''$) for Experiment No. 362016 [3].

domain analyses is that the enormous amount of algebra needed for linearization of equations, Laplace transformation, followed by obtaining expressions for transfer functions or transfer ratios is avoided. Here, linearization is performed numerically by the computer. This is followed by manipulation of large coefficient matrices, again by computer, to obtain the required frequency responses.

A problem that was encountered initially and eventually solved involved ill-conditioned coefficient matrices. It was found to be very important to monitor the condition number of various matrices such as those on the LHS of equations (23) and (24) when obtaining solutions.

Finally, it should be noted that the transfer functions reported in this work are the closed-loop ones. In order to obtain system stability information in the frequency domain via gain and phase calculations, it would be necessary to determine the corresponding open-loop transfer functions. This was not attempted in the present study.

Acknowledgements—This work was supported by Electric Power Research Institute, Nuclear Power Division, under research project RP 495-2.

REFERENCES

1. R. C. Dykhuizen, R. P. Roy and S. P. Kalra, A linear time-domain two-fluid model analysis of dynamic instability in boiling flow systems, *Trans. Am. Soc. Mech. Engrs*, Series C, *J. Heat Transfer* **108**, 100–108 (1986).
2. Y. Takahashi, M. J. Rabins and D. M. Auslander, *Control and Dynamic Systems*. Addison-Wesley, Reading, MA (1970).
3. O. Nylund *et al.*, FRIGG loop project, ASEA Atom, Sweden (1968).
4. H. Christensen, Power to void transfer function, ANL-6385 (1961).
5. G. C. Park, M. Podowski, M. Becker and R. T. Lahey, Jr., The Development of NUFREQ-N, an analytical model for the stability analysis of nuclear-coupled density-wave oscillation in boiling water reactor, NUREG/CR-3375 (1983).
6. N. Zuber and F. W. Staub, The propagation and waveform of the vapor volumetric concentration in boiling, forced convection system under oscillating condition, *Int. J. Heat Mass Transfer* **9**, 871–895 (1966).
7. F. W. Staub, N. Zuber and G. Bijwaard, Experimental investigation of the transient response of the volumetric concentration in a boiling forced flow system, *Nucl. Sci. Engng* **30**, 279–295 (1967).
8. F. W. Paul, K. J. Riedle and S. W. Gouse, Jr., Dynamics of two-phase flow, ONR Technical Report No. 1, Carnegie-Mellon University (1970).
9. R. G. Dorsch, Frequency response of forced flow single tube boiler, *Proc. Symposium on Two-Phase Flow Dynamics*, Eindhoven, The Netherlands (1967).
10. P. Saha and N. Zuber, An analytical study of the thermally induced two-phase flow instabilities including the effect of thermal non-equilibrium, *Int. J. Heat Mass Transfer* **21**, 415–421 (1978).
11. M. Ishii, *Thermo-fluid Dynamic Theory of Two-phase Flow*. Eyrolles, Paris (1975).
12. R. P. Roy and S. Ho, An unequal velocity, unequal temperature two-fluid description of transient vapor–liquid flow in channels, *Nucl. Sci. Engng* **81**, 459–467 (1982).
13. J. H. Stuhmiller, The influence of interfacial pressure forces on the character of two-phase flow model equations, *Int. J. Multiphase Flow* **3**, 551–560 (1977).
14. D. Drew, L. Cheng and R. T. Lahey, Jr., The analysis of virtual mass effects in two-phase flow, *Int. J. Multiphase Flow* **5**, 233–242 (1979).
15. C. W. Solbrig, J. H. McFadden, R. W. Lyczkowski and E. D. Hughes, Heat transfer and friction correlations required to describe steam–water behavior in nuclear safety studies, Fifteenth National Heat Transfer Conference, San Francisco (1975).
16. T. Sato and H. Matsumura, On the condition of incipient subcooled boiling with forced convection, *Bulletin J.S.M.E.* **7**, 392–398 (1964).
17. P. Saha, Thermally induced two-phase flow instabilities including the effect of thermal nonequilibrium between the phases. Ph.D. thesis, Georgia Institute of Technology (1974).
18. G. B. Wallis, *One-dimensional Two-phase Flow*. McGraw-Hill, New York (1969).
19. L. S. Tong, Boiling crisis and critical heat flux, AEC Critical Review Series (1972).
20. TRAC-P1A, An advanced best-estimate computer program for PWR LOCA analysis, NUREG/CR-0065, LA-7777-MS (1979).
21. J. H. Keenan, F. G. Keyes, P. G. Hill and J. G. Moore, *Steam Table (SI Units)*. Wiley, New York (1978).
22. P. J. Roache, *Computational Fluid Dynamics*, Hermosa, Albuquerque, NM (1976).
23. R. C. Dykhuizen, R. P. Roy and S. P. Kalra, Numerical method for solution of simultaneous nonlinear equations and application to two-fluid model equations of boiling flow, *Numer. Heat Transfer* **7**, 225–234 (1984).
24. M-G. Su, Frequency response of boiling flow systems based on a two-fluid model. M.Sc. thesis, Department of Mechanical and Aerospace Engineering, Arizona State University (1985).

REPONSE EN FREQUENCE DE SYSTEMES EN ECOULEMENT AVEC EBULLITION, A PARTIR D'UN MODELE A DEUX FLUIDES

Résumé—Un modèle à paramètre distribué de systèmes en écoulement avec ébullition est présenté. Il est construit à partir d'un modèle á domaine de temps linéarisé et à deux fluides, par la méthode du vecteur état-espace. Pour démontrer la validité de cette approche, des fonctions de transfert calculées par ce modèle sont comparées avec des solutions analytiques et des mesures expérimentales.

FREQUENZVERHALTEN VON SYSTEMEN MIT STRÖMUNGSSIEDEVORGÄNGEN AUF DER BASIS EINES ZWEIFLUIDMODELLS

Zusammenfassung—Ein Modell im Frequenzbereich mit verteilten Parametern für Systeme mit Strömungssiedevorgängen wird vorgestellt. Dieses wird aus einem linearisierten Zweifluidmodell im Zeitbereich mit Hilfe der Zustandsraum-Vektormethode entwickelt. Um die Gültigkeit dieser Näherung zu zeigen, werden die Übertragungsfunktionen, die von diesem Modell berechnet werden, mit analytischen Lösungen und experimentellen Werten verglichen.

ЧАСТОТНАЯ ХАРАКТЕРИСТИКА СИСТЕМ КИПЯЩЕГО ПОТОКА, ОСНОВАННЫХ НА ДВУХЖИДКОСТНОЙ МОДЕЛИ

Аннотация—Представлена модель с распределенным параметром для систем кипящего потока в частотной области. Она строится из линеаризованной двухжидкостной модели с помощью векторного метода. Для проверки справедливости данного подхода функции переноса, рассчитанные по этой модели, сравниваются с аналитическими решениями и экспериментальными данными.